

Micro Water-Energy Nexus: Optimal Demand-Side Management and Quasi-Convex Hull Relaxation

Qifeng Li, *Member, IEEE*, Suhyoun Yu, Ameena S. Al-Sumaiti, and Konstantin Turitsyn, *Member, IEEE*

Abstract—This paper investigates the water network’s potential ability to provide demand response services to the power grid under the framework of a distribution-level water-energy nexus (micro-WEN). In particular, the hidden controllability of water loads, such as irrigation systems, was closely studied to improve the flexibility of electrical grids. A optimization model is developed for the demand-side management (DSM) of micro-WEN, and the simulation results assert that grid flexibility indeed benefits from controllable water loads. Although the proposed optimal DSM model is an intractable mixed-integer nonlinear programming (MINLP) problem, quasi-convex hull techniques were developed to relax the MINLP into a mixed-integer convex programming (MICP) problem. The numerical study shows that the quasi-convex hull relaxation is tight and that the resulting MICP problem is computationally efficient.

Index Terms—Convex hull, convex relaxation, demand response, microgrid, water-energy nexus

I. INTRODUCTION

MODERN day water and power systems are closely intertwined as a coupled system, commonly referred to as the water-energy nexus (WEN) [1]–[5]. On one hand, most of the water facilities consume electrical energy. For instance, ground water pumping and seawater desalination account for roughly 12% of the total electric energy consumption in the Arabian Gulf regions [2]. On the other hand, water usage is inevitable in refining fuels and generating electric power. Despite the two networks’ inevitable interdependency, water and energy networks have traditionally been operated independently from one another, and the idea of co-operating the two in parallel has long been glossed over.

In recent years, researchers have started to direct their attention to water system’s potential ability to provide demand response (DR) services [6]. It is believed that higher cost-efficiency can be achieved by co-operating the water and power systems¹. In 2016, PG&E built up an efficiency partnership with the water utility in the city of San Luis Obispo which is the first-of-its-kind². The power sector suffers from an

unprecedented amount of network uncertainty with the ever-increasing penetration of intermittent renewable energy and electro-mobility [7], and the idea of exploiting the flexibility of water network has come under the spotlight as a possible solution. The co-operation of two systems allows the water system to fast and accurately response to the energy imbalance caused by the uncertain renewable energy generation or even contingencies on the electricity side. With this solution, the overall security and reliability of water and power systems will benefit from the nexus operation mode.

This paper focuses on developing a mathematical tool to assess the flexibility and responsiveness of a given micro-WEN, wherein both the water and energy networks are at distribution levels, to the energy imbalance. The AC power flow integrated with battery energy storage systems (BESSs) and high penetration of renewable energy sources [8] is used in the developed mathematical model. The water pipe network model is characterized by the directed Darcy-Weishach equation [9] and allow for water flow directions to reverse, and the on/off status of pumps are represented by integer variables. The resulting mathematical model for the micro-WEN is unfortunately a nonlinear mixed-integer model. To mitigate its intractability, a quasi-convex hull relaxation [8], [10] that is sufficiently tight and efficient is developed for the micro-WEN model.

Much of the micro-WEN’s flexibility will rise from the water sector, as electricity-driven water services—pumping, cooling, desalination, water treatment—are time-flexible. Further flexibility can be introduced by including controllable water loads such as irrigation services, which this paper uses to demonstrate hidden DR capabilities of the water network. The flexibility of pumps is constrained by water tank capacities that are physically limiting by nature, but incorporating controllable discharge scheme for water tanks should resolve the issue. Moreover, pumps, tanks and irrigation systems are to be jointly used to create virtual energy storages to power grids to alleviate the stress on the WEN in case of limited energy supply.

II. PROBLEM FORMULATIONS

A. Physical Model of Micro-WEN

The schematic of the micro-WEN is given in Figure 1. The electricity side is a distribution network, or a micro-grid, integrated with renewable energy and BESSs. The water side consists of a pipe network, pumps, utility- and customer-owned tanks and irrigation systems. EV’s and water treatment facilities—including desalination, water and waste water

This work is supported by the MI-MIT Cooperative Program under grant MM2017-000002.

Q. Li, S. Yu, and K. Turitsyn are with the Department of Mechanical Engineering, Massachusetts Institute of Technology, Cambridge, MA, 02139 USA, e-mail: {qifengli, syu2, turitsyn}@mit.edu.

A. Al-Sumaiti is with the Department of Electrical Engineering & Computer Science, Masdar Institute, Khalifa University of Science and Technology, Abu Dhabi, UAE, e-mail: aalsumaiti@masdar.ac.ae

¹California water utilities stake out new role in energy programs to finance their future, available at <http://artemiswaterstrategy.com/slopgepartnership/>.

²First-of-its-kind efficiency partnership with PG&E expected to save SLO millions in energy bills, available at <http://kcbx.org/post/first-its-kind-efficiency-partnership-pge-expected-save-slo-millions-energy-bills/#stream/0>.

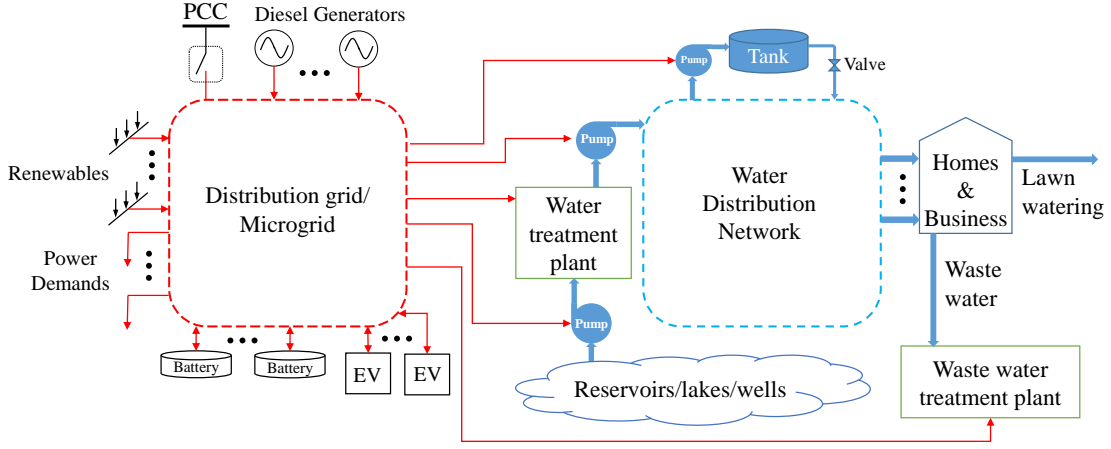


Figure 1. A physical structure of the micro water-energy nexus.

treatment and recycling—are not considered for the sake of simplicity, but those two elements can be easily incorporated and will be considered in future research.

It has been discussed in [1] that such a micro-WEN is a fundamental infrastructure of a smart building/city/village. Under the environment of smart buildings [11]/cities [12]/villages [13], all infrastructures will be connected through the emerging Internet of Things techniques. In order to operate and control such a connected physical system, it is essential to develop the mathematical model and design the optimization algorithms for optimal resource allocation.

B. Mathematical Model of Micro-WEN

This section introduces a multi-period mathematical model of the micro-WEN. Unless otherwise stated, the subscript t denotes the discrete time period. The structure of an AC-microgrid or an electric distribution system is usually radial. Consequently, we use a *DistFlow* model [14] integrated with renewable generation and batteries to describe the electricity network. The detailed model is given as

$$P_{i,t}^G + P_{i,t}^{RE} - P_{i,t}^{Pump} - P_{i,t}^L + P_{i,t}^{ES} = r_{ij} \mathcal{I}_{ji,t} - P_{ji,t} + \sum_{k \in \mathcal{D}_i} P_{ik,t} \quad (1a)$$

$$Q_{i,t}^G + Q_{i,t}^{RE} - Q_{i,t}^{Pump} - Q_{i,t}^L + Q_{i,t}^{ES} = x_{ij} \mathcal{I}_{ji,t} - Q_{ji,t} + \sum_{k \in \mathcal{D}_i} Q_{ik,t} \quad (1b)$$

$$\mathcal{V}_{i,t} - \mathcal{V}_{k,t} + (r_{ik}^2 + x_{ik}^2) \mathcal{I}_{ik,t} = 2(r_{ik} P_{ik,t} + x_{ik} Q_{ik,t}) \quad (1c)$$

$$P_{ik,t}^2 + Q_{ik,t}^2 = \mathcal{V}_{i,t} \mathcal{I}_{ik,t}, \quad (ik \in \mathcal{E}_E) \quad (1d)$$

$$P_{ik,t}^2 + Q_{ik,t}^2 \leq \bar{S}_{ik}^2, \quad (ik \in \mathcal{E}_E) \quad (1e)$$

$$0 \leq \mathcal{I}_{ik,t} \leq \bar{\mathcal{I}}_{ik}, \quad (1f)$$

$$\underline{\mathcal{V}}_i \leq \mathcal{V}_{i,t} \leq \bar{\mathcal{V}}_i \quad (1g)$$

$$\underline{P}_i^G, \underline{Q}_i^G \leq P_{i,t}^G, Q_{i,t}^G \leq \bar{P}_i^G, \bar{Q}_i^G, \quad (1h)$$

where $i \in \mathcal{N}_E$ and $ik \in \mathcal{E}_E$. For the sake of simplicity, this paper only consider the balanced cases. It has been proved in literature that the convex relaxations of the *DistFlow* for balanced networks can be easily extended to the unbalanced cases

under some mild approximations. Therefore, the proposed approach in this paper can be easily leveraged to the cases of three-phase unbalanced distribution networks or microgrids.

The following nonlinear model of a battery energy storage unit is incorporated into the overall mathematical model of the micro-WEN. Please refer to [8] for more details about this BESS model. For $\forall i \in \mathcal{N}_E^S$, we have

$$(r_i^{Batt} + r_i^{Cvt})(P_{i,t}^{ES})^2 + r_i^{Cvt}(Q_{i,t}^{ES})^2 = L_{i,t}^{ES} \mathcal{V}_{i,t} \quad (2a)$$

$$(P_{i,t}^{ES})^2 + (Q_{i,t}^{ES})^2 \leq (\bar{S}_i^{ES})^2 \quad (2b)$$

$$\underline{E}_i^{ES} \leq E_{i,0}^{ES} - \sum_{t=0}^t (P_{i,t}^{ES} + L_{i,t}^{ES}) \leq \bar{E}_i^{ES}. \quad (2c)$$

We make the following assumptions for the water distribution networks: (1) The pipe network is a directed graph $\mathcal{G}_W = (\mathcal{N}_W, \mathcal{E}_W)$ with incidence matrix A such that $A_{ik} \in \{-1, 0, 1\}$ for all i, k ; (2) A pump is considered as a type of pipe that imposes a head gain when the pump is on and closed otherwise; (3) The pump converts the electric power into a mechanical power at a constant efficiency of η ; (4) The power factors of pumps are fixed, namely $P_{k,t}^{Pump} / Q_{k,t}^{Pump}$ is constant. The resulting model can be expressed as:

$$\sum_{k \in \mathcal{E}_W} A_{ik} f_{k,t} = f_{i,t}^G - f_{i,t}^{UT} - f_{i,t}^{CT}, \quad (i \in \mathcal{N}_W) \quad (3a)$$

$$y_{i,t} - y_{j,t} + h_i - h_j = R_k^P \text{sgn}(f_{k,t}) f_{k,t}^2, \quad (k \in \mathcal{E}_W \setminus \mathcal{E}_W^P) \quad (3b)$$

$$\begin{cases} y_{i,t} - y_{j,t} + h_i - h_j \\ + y_{k,t}^G = R_k^P f_{k,t}^2 \\ f_{k,t} = 0, \end{cases} \quad \text{if } \alpha_{k,t} = 1, \quad (k \in \mathcal{E}_W^P) \quad (3c)$$

$$y_{k,t}^G = B_k f_{k,t} + C_k \quad (k \in \mathcal{E}_W^P) \quad (3d)$$

$$\underline{S}_i^w \leq S_{i,0}^w + \sum_{t=0}^t w_{i,\tau}^{UT} \leq \bar{S}_i^w, \quad (i \in \mathcal{N}_W^S) \quad (3e)$$

$$\underline{f} \leq f_t \leq \bar{f}, \quad (3f)$$

$$\underline{y} \leq y_t \leq \bar{y}, \quad (3g)$$

$$\underline{w}_i^G \leq w_{i,t}^G \leq \bar{w}_i^G, \quad (i \in \mathcal{N}_W^G) \quad (3h)$$

$$\underline{w}_i^S \leq w_{i,t}^S \leq \bar{w}_i^S, \quad (i \in \mathcal{N}_W^S) \quad (3i)$$

where A is a $|\mathcal{N}_W| \times |\mathcal{E}_W|$ incidence matrix and pipe k connects nodes i and j . Equation (3a) represents the mass balance of the water network; constraints (3b) and (3c) formulate the hydraulic characteristics of a normal pipe and the pipe with a pump installed respectively; constraint (3e) denotes the state of charging of the water tanks; (3f)-(3i) are system constraints; $\text{sgn}(f) = -1$ if $f \leq 0$ or, otherwise $\text{sgn}(f) = 1$. When $\alpha_{k,t} = 1$, the quantity $f_{k,t}$ in constraint (3c) is nonnegative. In model (3), the quantity $w_{i,t}^{CT}$ represents the uncontrollable water load. Similar to the uncontrollable electric load, it is a given value at each period.

The pumps are considered as constant-speed motors in this paper. The hydraulic characteristics of a constant-speed pump is generally approximated by a quadratic function of the water flow across the pump, i.e. $y^G = a_2 f^2 + a_1 f + a_0$ [17] and [18]. Contribution of the nonlinear $a_2 f^2$ is usually very small compared to the linear ones $a_1 f + a_0$. Thus, equation (3d) captures the head gain of a pump simply making $a_2 = 0$. The following constraints act as the mathematical link between the distribution network (1)-(2) and the WDS (3):

$$\eta P_{i,t}^{\text{Pump}} = f_{k,t} y_{k,t}^G = a_{1,k} f_{k,t}^2 + a_{0,k} f_{k,t}, \quad (4)$$

where $i \in \mathcal{N}_E^P$ and $k \in \mathcal{E}_W^P$.

C. A Co-optimization Framework of Water and Electricity

Based on the mathematical model of the micro-WEN introduced above, this subsection introduces a co-optimization framework for water and energy networks. The objective of this co-optimization problem is to minimize the total energy cost for meeting the demands of both electricity and water. We formulate the energy cost as

$$C(P_{i,t}^G) = \sum_t (c_t P_{1,t}^G + \sum_{i \in \mathcal{N}_E^G / \text{PCC}} (c_{1,i} P_{i,t}^G + c_{2,i} (P_{i,t}^G)^2)), \quad (5)$$

where $P_{1,t}^G$ denotes the power from the grid via PCC (i.e. the serial number of PCC is 1); c_t can be considered as the nodal prices at PCC which are obtained by solving the security constrained economic dispatch (SCED) by ISOs/RTOs. As a result, the co-optimization model is

$$\begin{aligned} \min_{P_{i,t}^G} \quad & (5) \\ \text{s.t.} \quad & (1) - (4) \end{aligned} \quad (\text{CO-OPT})$$

which is a mixed-integer nonlinear programming (MINLP).

III. QUASI-CONVEX HULL RELAXATIONS

The MINLP problem is computationally intractable, especially for large-scale systems. To reduce the computational burden, this section relaxes the MINLP into a mixed-integer convex programming problem [19] with high-tightness.

A. Convex Hull Relaxations of Constraints (1d) and (2a)

Within the circular bounds (1e) and (2b), the feasible sets of equations (1d) and (2a) can be captured by the following general formulation:

$$\Omega_0 = \left\{ x \mid \begin{array}{l} ax_1^2 + bx_2^2 = x_3 x_4 \\ x_1^2 + x_2^2 \leq c \\ \underline{x}_3, \underline{x}_4 \leq x_3, x_4 \leq \bar{x}_3, \bar{x}_4 \end{array} \right\}$$

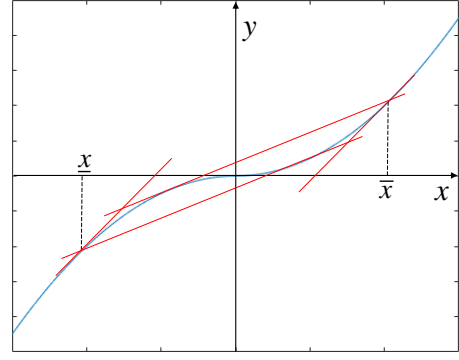


Figure 2. The quasi-convex hull of the hydraulic characteristic of a normal pipe.

where $x = [x_1 \ x_2 \ x_3 \ x_4]^T$, $a \geq b$, and $\underline{x}_3 \underline{x}_4 \leq c \leq \bar{x}_3 \bar{x}_4$. By generalizing the theorem presented in [8], we have the following Lemma.

Lemma. The convex hull of nonconvex set Ω_0 is

$$\Omega_1 = CH(\Omega_0) = \left\{ x \mid \begin{array}{l} ax_1^2 + bx_2^2 \leq x_3 x_4 \\ (a-b)x_2^2 + \underline{x}_4 x_3 \leq ac \\ (a-b)x_2^2 + \underline{x}_3 x_4 \leq ac \\ D^T x - d \leq 0 \\ x_1^2 + x_2^2 \leq c \\ \underline{x}_3, \underline{x}_4 \leq x_3, x_4 \leq \bar{x}_3, \bar{x}_4 \end{array} \right\}$$

where $D = [0 \ 0 \ k_1 \ k_2]^T$ is a coefficient vector, d is a scalar, and their values are given by

$$\begin{cases} k_1 = ac, k_2 = \underline{x}_3 \bar{x}_3, d = ac(\underline{x}_3 + \bar{x}_3) & \text{if } \bar{x}_3 \underline{x}_4 \leq ac \leq \underline{x}_3 \bar{x}_4 \\ k_1 = \underline{x}_4 \bar{x}_4, k_2 = ac, d = ac(\underline{x}_4 + \bar{x}_4) & \text{if } \underline{x}_3 \bar{x}_4 \leq ac \leq \bar{x}_3 \underline{x}_4 \\ k_1 = \underline{x}_4, k_2 = \underline{x}_3, d = ac + \underline{x}_3 \underline{x}_4 & \text{if } \bar{x}_3 \underline{x}_4, \underline{x}_3 \bar{x}_4 \leq ac \\ k_1 = \bar{x}_4, k_2 = \bar{x}_3, d = ac + \bar{x}_3 \bar{x}_4 & \text{if } ac \leq \bar{x}_3 \underline{x}_4, \underline{x}_3 \bar{x}_4 \end{cases}$$

Proof: See appendix. \square

For the case of (1d), $a = b = 1$, $c = \bar{S}_{ik}^2$, and $(\underline{x}_3, \underline{x}_4, \bar{x}_3, \bar{x}_4) = (\underline{\mathcal{V}}_i, 0, \bar{\mathcal{V}}_i, \bar{\mathcal{L}}_{ik})$, assume that $\bar{S}_{ik}^2 \leq \underline{\mathcal{V}}_i \bar{\mathcal{L}}_{ik}$. Within the system bounds (1e) - (1g), the convex hull of (1d) is given as

$$\begin{cases} P_{i,t}^2 + Q_{i,t}^2 \leq \mathcal{V}_{i,t} \bar{\mathcal{L}}_{i,t} \\ \bar{S}_{ik}^2 \mathcal{V}_i + \underline{\mathcal{V}}_i \bar{\mathcal{V}}_i \bar{\mathcal{L}}_{i,t} \leq \bar{S}_{ik}^2 (\underline{\mathcal{V}}_i + \bar{\mathcal{V}}_i) \end{cases} \quad (6)$$

For the case of (2a), $a = r_i^{\text{Batt}} + r_i^{\text{Cvt}}$, $b = r_i^{\text{Cvt}}$, $c = (\bar{S}_i^{\text{ES}})^2$, and $(\underline{x}_3, \underline{x}_4, \bar{x}_3, \bar{x}_4) = (\underline{\mathcal{V}}_i, 0, \bar{\mathcal{V}}_i, +\infty)$. It is obvious that $\bar{\mathcal{V}}_i \bar{\mathcal{L}}_{i,t}^{\text{ES}} \leq (\bar{S}_i^{\text{ES}})^2 (r_i^{\text{Batt}} + r_i^{\text{Cvt}}) \leq \underline{\mathcal{V}}_i \bar{\mathcal{L}}_{i,t}^{\text{ES}}$. Hence, within the system bounds (1g) and (2b), the convex hull of (2a) is

$$\begin{cases} (r_i^{\text{Batt}} + r_i^{\text{Cvt}})(P_{i,t}^{\text{ES}})^2 + r_i^{\text{Cvt}}(Q_{i,t}^{\text{ES}})^2 \leq \bar{\mathcal{L}}_{i,t}^{\text{ES}} \mathcal{V}_{i,t} \\ r_i^{\text{Batt}}(Q_{i,t}^{\text{ES}})^2 + \underline{\mathcal{V}}_i \bar{\mathcal{L}}_{i,t}^{\text{ES}} \leq (\bar{S}_i^{\text{ES}})^2 (r_i^{\text{Batt}} + r_i^{\text{Cvt}}) \\ (\bar{S}_i^{\text{ES}})^2 \mathcal{V}_i + \underline{\mathcal{V}}_i \bar{\mathcal{V}}_i \bar{\mathcal{L}}_{i,t}^{\text{ES}} \leq (\bar{S}_i^{\text{ES}})^2 (\underline{\mathcal{V}}_i + \bar{\mathcal{V}}_i) \end{cases} \quad (7)$$

B. Quasi-Convex Hull Relaxation of (3b)

With the left-hand-side replaced by an auxiliary variable y and the right-hand-side replaced by a general term $R^P \text{sgn}(f) f^2$, function (3b) yields the blue curve, as shown in Figure 2, in the (f, y) -plane. It is relaxed into the red polygon

as shown in the figure. The red polygon is not exactly the convex hull of (3b). However, it is very close to the convex hull from the perspective of tightness and, therefore, is called a quasi-convex hull. Its mathematical formulation is given as

$$y_{i,t} - y_{j,t} + h_i - h_j \begin{cases} \leq (2\sqrt{2} - 2)R_k^P \bar{f}_k f_{k,t} + (3 - 2\sqrt{2})R_k^P \bar{f}_k^2 \\ \geq (2\sqrt{2} - 2)R_k^P \underline{f}_k f_{k,t} + (3 - 2\sqrt{2})R_k^P \underline{f}_k^2 \\ \geq 2R_k^P \bar{f}_k f_{k,t} - R_k^P \bar{f}_k^2 \\ \leq 2R_k^P \underline{f}_k f_{k,t} - R_k^P \underline{f}_k^2 \end{cases} \quad (8)$$

C. Convex Hull Relaxation of Constraint (3c)

The nonconvex constraint (3c) contains a logic proposition. To eliminate the if expression, we use the big- M technique to rewrite constraint (3c) as

$$R_k^P f_{k,t}^2 - Y_1 \leq 0 \quad (9a)$$

$$Y_2 - R_k^P f_{k,t}^2 \leq 0 \quad (9b)$$

$$0 \leq f_{k,t} \leq M * \alpha \quad (9c)$$

where $Y_1 = y_{i,t} - y_{j,t} + h_i - h_j + y_{k,t}^G + M * (1 - \alpha)$ and $Y_2 = y_{i,t} - y_{j,t} + h_i - h_j + y_{k,t}^G + M * (\alpha - 1)$. Note that the expression (9a) is convex, while (9b) is a concave constraint. The convex hull of (9b) can be obtained through a geometric approach as shown in Figure 3. Its mathematical expression is given as

$$Y_2 - R_k^P \bar{f}_k f_{k,t} \leq 0. \quad (10)$$

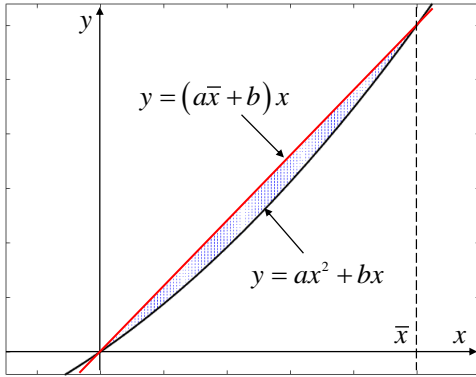


Figure 3. Convex hull of a parabola.

It can be observed, by comparing Figures 2 and 3, that one can construct a tighter relaxation for the hydraulic characteristic of a pipe if the direction of water flow is given. A planning problem of gas networks is discussed in [20] where the authors introduced additional binary variables and bilinear equations to relax the Weymouth equation. The Weymouth equation is similar to constraint (3b). However, the convex relaxation of the Weymouth equation developed in [20] is not necessarily tighter than the proposed relaxation (8) due to the introduced bilinear equations. Moreover, the auxiliary binary variables and constraints in [20] are not desirable for an operation problem which is sensitive to computational time.

D. Convex Hull Relaxation of Constraint (4)

Constraint (4) is a quadratic equation which can be considered as the intersection of a convex inequality and a concave inequality. The geometric approach introduced in Figure 3 can be used to construct the convex hull of the concave inequality. As a result, the convex hull constraint (4) is given by

$$\eta P_{i,t}^{\text{Pump}} \geq a_k f_{k,t}^2 + b_k f_{k,t} \quad (11a)$$

$$\eta P_{i,t}^{\text{Pump}} \leq (a_k \bar{f}_k + b_k) f_{k,t} \quad (11b)$$

where $f_{k,t}$ is nonnegative since the direction of pump flows is determined.

E. Quasi-Convex Hull Relaxation of (CO-OPT)

To sum up, the quasi-convex hull relaxation of the overall co-optimization problem (CO-OPT) is

$$\min \quad (5)$$

$$\text{s.t.} \quad (1a-c, e-i), (2b-c), (3a, d-i), (6) \quad (\text{C-CO-OPT})$$

$$(7), (8), (9a, c), (10) \text{ and } (11),$$

which is a mixed-integer convex quadratically-constrained quadratic programming (MICQCQP) problem.

The basic idea of the quasi-convex hull relaxation of an optimization problem is replacing the nonconvex constraints with their convex hulls or quasi-convex hulls. As discussed in [8], [10], the concept of convex hull is attractive since the extreme points of a convex hull generally belong to its original non-convex set. If the objective function is a convex function and monotonic over the convex hull, the optimal solution is usually located at one of the extreme points, implying that the optimal solution obtained by solving the convex relaxation is most likely the exact globally optimal solution of the original problem. Unfortunately, for many of the nonlinear nonconvex sets, it is extremely hard to formulate their convex hulls. For such cases, an interesting alternative is to construct a convex inner approximation of a nonconvex set [21]. Compared with the convex relaxation, the foremost advantage of the convex inner approximation is guaranteeing the feasibility of the obtained solutions to the original nonconvex set.

A characteristic of the MINLP problem (CO-OPT) is that the integer variables only exist in linear terms of constraints. For the purpose of improving the computational efficiency, it is wise to relax such a mixed-integer problem into a mixed-integer convex problem. The convex relaxations which are tight for the continuous cases are equivalently tight for the discrete cases since the nonconvex terms that need to be relaxed do not contain integer variables.

IV. A FLEXIBLE IRRIGATION SCHEME

A. Flexibility of Irrigation Systems

It is straightforward to improve the grid flexibility by allowing for controllability of electric loads. From a different angle, this subsection explores opportunities for improving the DR capacity of water systems by investigating the flexibility of customer-owned water tanks and irrigation systems which are water loads rather than electric loads. An intuitive interpretation is that customers can use the superfluous energy to

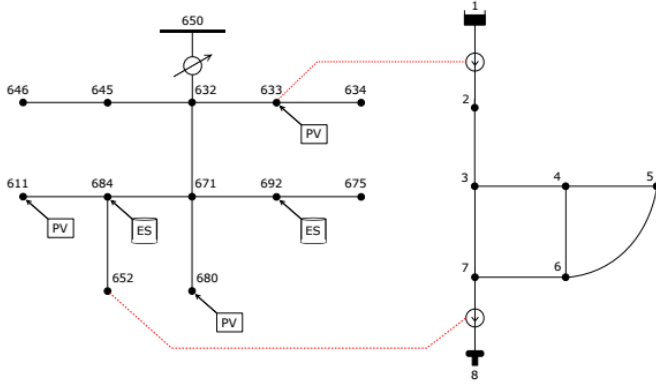


Figure 4. Topology of the test system.

pump and store water. However, there are some certain volume limits on tanks. Thus, it is necessary to develop a coordination strategy for charging and discharging tanks based on the multi-period energy imbalance and the flexible water consumption.

Assuming that the crops growth is not sensitive to the watering time, the irrigation process is considered flexible. To develop a mathematical model of such a flexible irrigation system, we have the following assumptions: i) the irrigation flow is fixed and the irrigation volume is a function of the watering time; ii) for a given season, the total amount of water is fixed, which can be represented as turning on the irrigation system for totally N hours per day. Consequently, the mathematical model is given by

$$\underline{S}_i^w \leq S_{i,0}^w + \sum_{t=0}^t (f_{i,t}^{CT} - f_{i,t}^D - k\alpha_{i,t}) \leq \bar{S}_i^w \quad (12a)$$

$$\sum_t \alpha_{i,t} = N, \quad (12b)$$

which are mixed-integer linear.

B. A Mixed-integer Convex DSM Scheme of Water Systems

By incorporating the model (12) of flexible irrigation systems into (C-CO-OPT), we have the following DSM scheme

$$\begin{aligned} \min \quad & (5) \\ \text{s.t.} \quad & (1a-c, e-i), (2b-c), (3a, d-i), (6) \\ & (7), (8), (9a, c), (10), (11) \text{ and } (12), \end{aligned} \quad (\text{C-DSM})$$

which is also an MICQCQP problem.

V. CASE STUDY

A. Introduction to the Test System

The micro-WEN for the case study is composed of the IEEE 13-bus system and an 8-node WDS from the EPANET manual [15]. The topology of the test micro-WEN is given in Figure 4. We assume that the 13-bus microgrid is integrated with high penetration of PV resources. Figure 4 shows the shape of a typical average load in summer [16]. The 24-hour load profile of the 13-bus system is generated by applying this load shape with the load provided by IEEE as the load at 9 am. Further

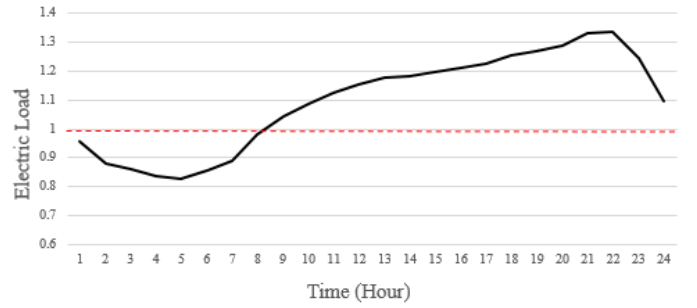


Figure 5. The shape of a typical average load in summer.

Table I
PV SYSTEM, BESS, AND PUMP PARAMETERS

PV location (bus #) and capacity	Penetration
633 (0.5 MW), 680 (0.2 MW), 684 (0.5 MW)	34.68%
BESS location (bus #) and capacity	
684 (1.15 MVA, 2.5 MWh), 692 (1.41 MVA, 3.2 MWh)	
Pump location (bus #) and parameters	
633 ($b=0.3$ p.u., $c=0.4$ p.u.), 652 ($b=0.3$ p.u., $c=0.4$ p.u.)	

detailed information about the PV systems, BESSs, and pumps are given in Table I.

Pumps deliver 30.48 meters and 15.24 meters of head respectively at a flow of $0.038 \text{ m}^3/\text{s}$. The tank is 18.3 meters in diameter and 5.1 meters in depth. For the 24-hour demand profiles and the lengths of pipes of the water system, please refer to the EPANET manual. The parameter R_{ij}^P is calculated by (the subscript ij is eliminated for the sake of simplicity)

$$R^P = \frac{8fL}{\pi^2 g D^5}$$

where f is the coefficient of surface resistance, D and L are the diameter and length of pipe respectively, and g is the gravitational acceleration.

B. Tightness of the QCH Relaxation

The tightness of the proposed convex relaxation is first evaluated by comparing solutions obtained by solving (CO-OPT) and (C-CO-OPT), respectively. Using the JuMP package of Julia [22], the optimization problems were solved in a MAC computer with a 64-bit Intel i7 dual core CPU at 2.40 GHz and 8 GB of RAM. The MINLP problem (CO-OPT) and its quasi-convex hull relaxation (C-CO-OPT) are solved by calling BONMIN [23] and GUROBI [24] solvers respectively.

The simulation results are tabulated in Table II. The first and foremost improvement brought by convexification is in the computational efficiency. The required CPU time has been significantly reduced by solving the quasi-convex hull relaxation. Note that BONMIN is an open source solver with a limited computational capacity. However, MINLP problems are NP-hard to solve. Even using some well-designed commercial solvers, like KNITRO [25], the CPU time of solving a MINLP problem is still not comparable to that of solving a MICQCQP problem of a similar size.

The proposed quasi-convex hull relaxation is exact for the test case in this paper. It means that the optimal solution

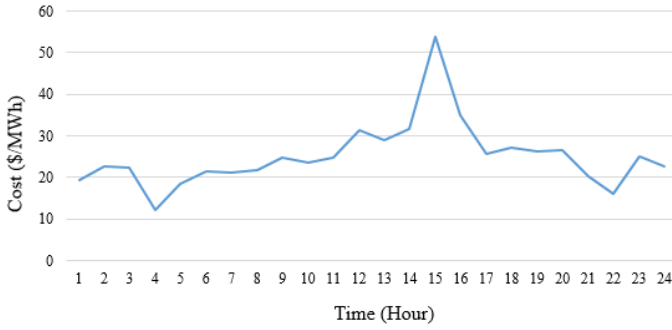


Figure 6. The 24-hour nodal price at PCC.

obtained by solving (C-CO-OPT) is the exact global optimal solution of its original nonconvex problem (CO-OPT) with zero optimality gap. The numerical results in this subsection demonstrate the potential of the proposed quasi-convex hull relaxation for convexifying similar MINLP problems with high-accuracy.

C. Improvement in System Security

In current practice, the electrical and water systems are operated separately by the electrical and water utilities respectively. First, the water utility tries to minimize the energy consumption by doing a day-ahead optimal pump scheduling based on the day-ahead water demand forecast (see the formulation (OPS) in [1]). Then, with the schedule of energy consumption reported by the water utility, the power operator solves a multi-period optimization problem (see the formulation (UC) in [1]) to minimize the total energy cost for meeting all electricity demands based on the day-ahead forecast of electricity demands, where the diesel generators and BESS units are control devices. It can be observed from Table III that the co-optimization produces a lower-cost solution under the same penetration level.

In this section, we also evaluate the improvement in system security introduced by co-optimizing the electrical and water networks. There is a certain limit on the penetration of PV that the distribution system can accommodate. A PV generation that exceed this limit will cause security problem to the system. The simulation results tabulated in Table III demonstrate that, by considering the pumps as controllable loads, the PV penetration which can be accommodated by the power distribution system is increased by 33%. In reality, the proposed co-operation scheme of micro-WEN allows the electricity-driven water facilities response to energy uncertainties in the power grid and, consequently, improve the system's security.

D. Efficiency of the DSM Scheme of Tanks

This subsection evaluates the efficiency for the demand response of the flexible irrigation system (12) by comparing the results of (C-CO-OPT) and (C-DSM). Both problems are MICQCQP and solved by GUROBI on the computer mentioned in the previous subsection. The results are tabulated in Table IV. Problem (C-DSM) has more integer decision variables than (C-CO-OPT). However, the CPU time for solving

(C-DSM) is not significantly larger than that for solving (C-CO-OPT) due to the property that the nonlinear terms are convex.

In the studied case, 30% of the total water load is for irrigation and, namely, flexible. It can be observed from Table IV that the total operational costs of the micro-WEN can be reduced by considering the flexibility of the irrigation systems. A considerable cost saving can be expected if: 1) the proposed approach is applied to a larger system, 2) the flexibility of other water facilities, such as water/waste water treatment, desalination, recycling, and cooling, is also included.

VI. CONCLUSION AND FUTURE WORK

This paper introduces a mixed-integer nonlinear mathematical model for the distribution-level water-energy nexus, or the micro-WEN. A co-optimization framework for water and energy distribution networks is built upon this mathematical model. Based on the convex hulls or quasi-convex hulls of the system components, a tight mixed-integer convex relaxation is developed to improve the computational efficiency of solving the co-optimization framework. When the proposed approach is applied to solve the co-optimization problem of a micro-WEN which consists of a 13-bus distribution system and an 8-node water distribution network, the CPU time reduces from nearly 2 hours to less than 1 second.

To further explore the capacity of water distribution systems for providing demand response service to the power grids, this paper developed an optimal demand response framework considering a flexible irrigation system. Simulation results on the test micro-WEN demonstrated the DR potential of water systems. In the future work, we will consider the flexibility of other water facilities, such as water/waste water treatment, desalination, recycling, and cooling, in the DSM model.

The water-energy nexus is a fundamental infrastructure in the building/city/village as both water and electricity are lifelines of humans. The findings of this research should be a good fit to the research framework of the smart building/city/village.

APPENDIX

The proof for only the case, where $k_1 = ac$, $k_2 = \underline{x}_3\bar{x}_3$, and $d = ac(\underline{x}_3 + \bar{x}_3)$ is provided due to the page limit. The set Ω_1 represents a convex solid, in the x -space, that consists of 5 (linear) facets and 4 (nonlinear) surfaces. The relation $\Omega_1 = CH(\Omega_0)$ means $CH(\Omega_0) \subseteq \Omega_1$ and $\Omega_1 \subseteq CH(\Omega_0)$.

(i) $CH(\Omega_0) \subseteq \Omega_1$

Let

$$\Omega_2 = \left\{ x \mid \begin{array}{l} ax_1^2 + bx_2^2 \leq x_3x_4 \\ x_1^2 + x_2^2 \leq c \\ \underline{x}_3, \underline{x}_4 \leq x_3, x_4 \leq \bar{x}_3, \bar{x}_4 \end{array} \right\}$$

$$\Omega_3 = \left\{ x \mid \begin{array}{l} (a-b)x_2^2 + \underline{x}_4x_3 \leq ac \\ x_1^2 + x_2^2 \leq c \\ \underline{x}_3, \underline{x}_4 \leq x_3, x_4 \leq \bar{x}_3, \bar{x}_4 \end{array} \right\}$$

$$\Omega_4 = \left\{ x \mid \begin{array}{l} (a-b)x_2^2 + \underline{x}_3x_4 \leq ac \\ x_1^2 + x_2^2 \leq c \\ \underline{x}_3, \underline{x}_4 \leq x_3, x_4 \leq \bar{x}_3, \bar{x}_4 \end{array} \right\}$$

Table II
RESULTS OF TIGHTNESS

Problem	Mathematical Classification	Solver	Optimal Solution (\$)	Optimality Gap	CPU Time
(CO-OPT)	MINLP	BONMIN	1463	-	≈ 2 hrs
(C-CO-OPT)	MICQCQP	GUROBI	1463	0	< 1 sec

Table III
CAPABILITY OF PV PENETRATION

Operation Scheme	Penetration Cap	Optimal Solution (\$)
Independent Optimization	83.23%	1579
Co-optimization	110.98%	1463

Table IV
RESULTS OF ECONOMIC EFFICIENCY

Problem	Mathematical Classification	Solver	Optimal Solution (\$)	CPU Time
(C-CO-OPT)	MICQCQP	GUROBI	1463	< 1 sec
(C-DSM)	MICQCQP	GUROBI	1455	< 1 sec

$$\Omega_5 = \left\{ x \mid \begin{array}{l} D^T x - d \leq 0 \\ x_1^2 + x_2^2 \leq c \\ \underline{x}_3, \underline{x}_4 \leq x_3, x_4 \leq \bar{x}_3, \bar{x}_4 \end{array} \right\},$$

which are convex sets. It is straight forward to know that $\Omega_0 \subseteq \Omega_2$. Under the condition $x_1^2 + x_2^2 \leq c$, equation $ax_1^2 + bx_2^2 = x_3x_4$ implies $(a-b)x_2^2 + x_3x_4 = a(x_1^2 + x_2^2) \leq ac$. Any point (x_2, x_3) that satisfies $(a-b)x_2^2 + x_3x_4 \leq ac$ will also satisfy $(a-b)x_2^2 + \underline{x}_4x_3 \leq ac$. Therefore, $\Omega_0 \subseteq \Omega_3$. Similarly, we can prove that $\Omega_0 \subseteq \Omega_4$. Equation $ax_1^2 + bx_2^2 = x_3x_4$ also implies $x_3x_4 \leq ac$ since $ax_1^2 + bx_2^2 \leq ac$. From Figure 7, it suffices to show that $\Omega_0 \subseteq \Omega_5$. The convex hull of Ω_0 is defined as the intersection of all convex relaxations of Ω_0 [26]. Hence, $CH(\Omega_0) \subseteq (\Omega_2 \cap \Omega_3 \cap \Omega_4 \cap \Omega_5) = \Omega_1$.

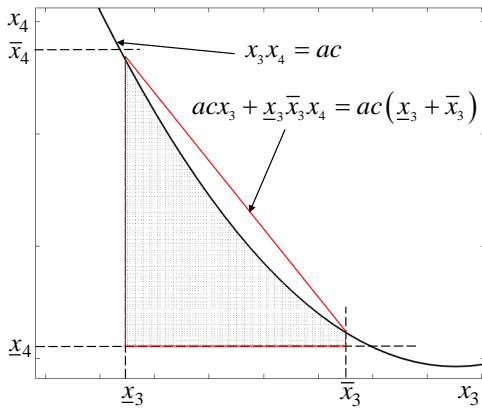


Figure 7. Convex hull relaxation of $x_3x_4 \leq ac$. The shaded area is the original nonconvex set while the trapezoid region with red boundaries is its convex hull.

(ii) $\Omega_1 \subseteq CH(\Omega_0)$

If a linear cut is valid for the convex set $CH(\Omega_0)$, it will also be valid for any subset of $CH(\Omega_0)$. Note that “a linear inequality is valid for a set” means the inequality is satisfied by all its feasible solutions [27]. On the other hand, Ω_1 is a

subset of $CH(\Omega_0)$ if any valid cut of $CH(\Omega_0)$ is also valid for Ω_1 according to the properties of supporting hyperplanes [26]. Let $\alpha^T x \leq \beta$ denote any given valid linear cut for $CH(\Omega_0)$, it should also be valid for Ω_0 . The cut $\alpha^T x \leq \beta$ is valid for Ω_1 if it is valid for all the surfaces of Ω_1 .

The mathematical formulation of a surface can be obtained by changing one inequality constraint in Ω_1 into an equality. For instance, Surf_1 and Surf_2 are two surfaces of solid Ω_1 . It is straight forward to show that $\alpha^T x \leq \beta$ is valid for Surf_1 since, in reality, $\text{Surf}_1 = \Omega_0$. In this appendix, we prove that $\alpha^T x \leq \beta$ is valid for Surf_2 as an example.

$$\text{Surf}_1 = \left\{ x \mid \begin{array}{l} ax_1^2 + bx_2^2 = x_3x_4 \\ (a-b)x_2^2 + \underline{x}_4x_3 \leq ac \\ (a-b)x_2^2 + \underline{x}_3x_4 \leq ac \\ D^T x - d \leq 0 \\ x_1^2 + x_2^2 \leq c \\ \underline{x}_3, \underline{x}_4 \leq x_3, x_4 \leq \bar{x}_3, \bar{x}_4 \end{array} \right\}$$

$$\text{Surf}_2 = \left\{ x \mid \begin{array}{l} ax_1^2 + bx_2^2 \leq x_3x_4 \\ (a-b)x_2^2 + \underline{x}_4x_3 = ac \\ (a-b)x_2^2 + \underline{x}_3x_4 \leq ac \\ D^T x - d \leq 0 \\ x_1^2 + x_2^2 \leq c \\ \underline{x}_3, \underline{x}_4 \leq x_3, x_4 \leq \bar{x}_3, \bar{x}_4 \end{array} \right\}$$

Let $\tilde{x} = (\tilde{x}_1, \tilde{x}_2, \tilde{x}_3, \tilde{x}_4)$ denote any given point on Surf_2 , where $(a-b)\tilde{x}_2^2 + \underline{x}_4\tilde{x}_3 = ac$. Let's consider the two chosen points $\hat{x}_1 = (\hat{x}_{1,1}, \tilde{x}_2, \tilde{x}_3, \hat{x}_{1,4})$ and $\hat{x}_2 = (\hat{x}_{2,1}, \tilde{x}_2, \tilde{x}_3, \hat{x}_{2,4})$ which are located in the original feasible set Ω_0 . That means $a\hat{x}_{i,1}^2 + b\tilde{x}_2^2 = \tilde{x}_3\hat{x}_{i,4}$ for $i = 1, 2$. By carefully choosing the values of $\hat{x}_{1,1}$ and $\hat{x}_{2,1}$ inside the required bounds, we can make conditions $\hat{x}_{1,1} \leq \tilde{x}_1 \leq \hat{x}_{2,1}$ and $\hat{x}_{1,4} \leq \tilde{x}_4 \leq \hat{x}_{2,4}$ hold. As a result, it suffices to show that the following condition holds:

$$\tilde{x} = \gamma_1 \hat{x}_1 + \gamma_2 \hat{x}_2$$

where γ_1 and γ_2 are nonnegative, and $\gamma_1 + \gamma_2 = 1$. There always exist two points \hat{x}_1 and \hat{x}_2 that satisfy the above conditions for any given point \tilde{x} on Surf_2 as long as the intersection of Ω_0 and Surf_2 is nonempty. In reality, Surf_2 is redundant if its intersection with Ω_0 is an empty set. We don't need to consider the case that Surf_2 is redundant.

Given that \hat{x}_1 and \hat{x}_2 belong to the original set Ω_0 , the linear cut $\alpha^T x \leq \beta$ is valid for both of them. Therefore, we have

$$\alpha^T \tilde{x} = \gamma_1 \alpha^T \hat{x}_1 + \gamma_2 \alpha^T \hat{x}_2 \leq \gamma_1 \beta + \gamma_2 \beta = \beta,$$

which means $\alpha^T x \leq \beta$ is also valid for \tilde{x} and, consequently, Surf_2 since \tilde{x} represents any point on Surf_2 . We do not provide the proof showing that the linear cut is also valid for

the rest of surfaces due to the page limit. The readers could to the proofs themselves by following the above method for the rest of surfaces of Ω_1 and the rest of the cases in the Lemma.

REFERENCES

- [1] Q. Li, S. Yu, A. Al-Sumaiti, and K. Turitsyn, "Modeling A Micro-Nexus of Water and Energy for Smart Villages/Cities/Buildings." arXiv preprint arXiv:1711.03241 (2017).
- [2] A. Siddiqi and L. Diaz Anadon, "The water–energy nexus in Middle East and North Africa." *Energy policy* 39, no. 8 (2011): 4529–4540.
- [3] X. Zhang, and V. V. Vesselinov, "Energy-water nexus: Balancing the tradeoffs between two-level decision makers." *Applied Energy* 183 (2016): 77–87.
- [4] A. Santhosh, A. M. Farid, and K. Youcef-Toumi, "Real-time economic dispatch for the supply side of the energy-water nexus." *Applied Energy* 122 (2014): 42–52.
- [5] A. Santhosh, A. M. Farid, and K. Youcef-Toumi, "Optimal network flow for the supply side of the energy-water nexus." In *Intelligent Energy Systems (IWIES), 2013 IEEE International Workshop on*, pp. 155–160. IEEE, 2013.
- [6] R. Menke, E. Abraham, P. Pappas, and I. Stoianov, "Demonstrating demand response from water distribution system through pump scheduling." *Applied Energy* 170 (2016): 377–387.
- [7] P. Palensky and D. Dietrich, "Demand side management: Demand response, intelligent energy systems, and smart loads," *IEEE Trans. Ind. Inform.*, vol. 7, no. 3, pp. 381–388, Aug 2011.
- [8] Q. Li, and V. Vittal, "Convex Hull of the Quadratic Branch AC Power Flow Equations and Its Application in Radial Distribution Networks." *IEEE Transactions on Power Systems* (2017).
- [9] M. H. Chaudhry, "*Applied Hydraulic Transients*", 3rd edition, New York: Springer-Verlag, 2014.
- [10] Q. Li, and V. Vittal, "The convex hull of the AC power flow equations in rectangular coordinates." In *Power and Energy Society General Meeting (PESGM), 2016*, pp. 1–5. IEEE, 2016.
- [11] B. Morvaj, L. Lugaric, and S. Krajcar. "Demonstrating smart buildings and smart grid features in a smart energy city," In *Proc. of the 2011 3rd International Youth Conference on Energetics (IYCE)*, IEEE, 2011.
- [12] V. Albino, U. Berardi, and R. Maria Dangelico. "Smart cities: Definitions, dimensions, performance, and initiatives." *Journal of Urban Technology*, vol. 22, no. 1, pp: 3–21, 2015.
- [13] R. B. Heap, "Smart villages: New thinking for off-grid communities worldwide." *Essay Compilation, Banson*, 2015.
- [14] M. E. Baran, and Felix F. Wu. "Optimal capacitor placement on radial distribution systems." *IEEE Transactions on power Delivery* 4, no. 1 (1989): 725–734.
- [15] L. A. Rossman, "EPANET 2: users manual." (2000).
- [16] D. Narang and C. Neuman, *High Penetration of Photovoltaic Generation Study – Flagstaff Community Power: Results of Phase 1*, DOE Final Technical Report, de-ee0002060, Sept. 2011.
- [17] B. Ulanicki, J. Kahler, and B. Coulbeck, "Modeling the efficiency and power characteristics of a pump group," *Journal of Water Resources Planning and Management*, vol. 134, no. 1, pp. 88–93, 2008.
- [18] D. Fooladivanda, and J. A. Taylor. "Optimal pump scheduling and water flow in water distribution networks." In *Decision and Control (CDC), 2015 IEEE 54th Annual Conference on*, pp. 5265–5271. IEEE, 2015.
- [19] P. Bonami, M. Kilinç, and J. Linderoth, "Algorithms and software for convex mixed integer nonlinear programs." In *Mixed integer nonlinear programming*, pp. 1–39. Springer, New York, NY, 2012.
- [20] C. Borraz-Sánchez, R. Bent, S. Backhaus, H. Hijazi, and P. Van Hentenryck. "Convex relaxations for gas expansion planning." *INFORMS Journal on Computing*, vol. 28, no. 4 (2016): 645–656.
- [21] H. D. Nguyen, K. Dvijotham, and K. Turitsyn, "Inner approximations of power flow feasibility sets," arXiv preprint arXiv:1708.06845 (2017).
- [22] C. Kwon, "Julia Programming for Operations Research: A Primer on Computing." CreateSpace Independent Publishing Platform, 2016.
- [23] I. Grossmann, P. Bonami, L. Biegler, A. Conn, G. Cornuejols, C. Laird, J. Lee et al. "An Algorithmic Framework for Convex Mixed Integer Nonlinear Programs," *IBM Research Report RC23771*, 2005.
- [24] Gurobi Optimization, "Gurobi Optimizer 5.0." Gurobi: <http://www.gurobi.com> (2013).
- [25] R. Byrd, J. Nocedal, and R. A. Waltz. "KNITRO: An integrated package for nonlinear optimization." In *Large-scale nonlinear optimization*, pp. 35–59. Springer US, 2006.
- [26] S. Boyd, and L. Vandenberghe. *Convex optimization*. Cambridge, UK: Cambridge University Press, 2004.
- [27] V. Borozan and G. Cornuejols, "Minimal valid inequalities for integer constraints," *Math. Oper. Res.*, vol. 34, no. 3, pp. 538–546, 2009.
- [28] M. Bazaraa, H. D. Sherali, and C. M. Shetty. *Nonlinear programming: theory and algorithms*. Hoboken, NJ: John Wiley & Sons, 2013.